

See discussions, stats, and author profiles for this publication at: <https://www.researchgate.net/publication/231229494>

# A New Bridging Chelating Ligand for Crystal Engineering: Synthesis, Polymorphism, and Two Modes of Assembly of 1,4-Bis(3-phenyl-1,3-propanedion)benzene with Metal Cations Resulting...

ARTICLE *in* CRYSTAL GROWTH & DESIGN · JUNE 2003

Impact Factor: 4.89 · DOI: 10.1021/cg030016b

---

CITATIONS

42

---

READS

142

5 AUTHORS, INCLUDING:



**Dmitriy Soldatov**

University of Guelph

**103** PUBLICATIONS **1,811** CITATIONS

SEE PROFILE



**John A. Ripmeester**

National Research Council Canada

**713** PUBLICATIONS **15,385** CITATIONS

SEE PROFILE

# A New Bridging Chelating Ligand for Crystal Engineering: Synthesis, Polymorphism, and Two Modes of Assembly of 1,4-Bis(3-phenyl-1,3-propanedion)benzene with Metal Cations Resulting in Either Discrete or Polymeric Complexes

D. V. Soldatov,<sup>\*,†,‡</sup> A. S. Zanina,<sup>§</sup> G. D. Enright,<sup>†</sup> C. I. Ratcliffe,<sup>†</sup> and J. A. Ripmeester<sup>†</sup>

*Steele Institute for Molecular Sciences, National Research Council of Canada, Ottawa K1A 0R6, Canada, Institute of Inorganic Chemistry, Siberian Branch of the Russian Academy of Sciences, Novosibirsk 630090, Russia, and Institute of Chemical Kinetics and Combustion, Siberian Branch of the Russian Academy of Sciences, Novosibirsk 630090, Russia*

Received April 4, 2003

**ABSTRACT:** This work introduces a new ligand ( $H_2L$ ,  $PhCOCH_2COPhCOCH_2COPh$ ) bearing two  $\beta$ -diketonate functions separated by a phenylene ring. The free ligand was synthesized and isolated in two polymorphic modifications. The ligand exhibits a preference for one of two basic conformational types where  $\beta$ -diketonate functions are approximately coplanar and directed either on opposite sides (trans) or on the same side ( $\sim 60^\circ$  to each other (cis)). In the free form, the ligand exists as 100% enol; in the solid state, it adopts a trans conformation. In a one-dimensional (1D) coordination polymer  $[ZnPy_2L]_n \cdot nPy$ , the ligand adopts the trans conformation and chelates to two zinc(II) centers bridging them at 11.3 Å. In three of the crystals studied, another structure was observed with an ideal formula  $[M_3Py_6L_3] \cdot 5(CHCl_3)$ . In this case, the ligand adopts a cis conformation and chelates to two metal centers bridging them at 10.7 Å, to produce a trinuclear macrocyclic species. In the crystal, these triangles pack to create channels that accommodate chloroform as a guest. The specific crystals studied had the following overall compositions:  $[Co_3Py_6L_3] \cdot 4.84(CHCl_3)$ ,  $[Co_3Py_6L_3] \cdot 4.11(CHCl_3)$ , and  $[Ni_3Py_6L_3] \cdot 4.68(CHCl_3)$ . The architecture displays flexibility and zeolite-like behavior.

## Introduction

Crystal engineering<sup>1</sup> is targeted at the predictable assembly of molecular species into extended architectures. Therefore, one of the most necessary tasks of current research is the synthesis of new building elements that have a programmed tendency to form supramolecular motifs of defined geometry.<sup>2–15</sup> Especially interesting are building elements that can trigger local environmental shifts between two stable states and thus have potential for the production of switchable and smart materials.<sup>16–18</sup>

Bridging ligands have been extensively utilized to produce a great number of supramolecular coordination species and frameworks; most common are cyanide<sup>19–22</sup> and 4,4'-bipyridyl,<sup>23,24</sup> which connect to each metal center with a single donor atom. Chelating ligands provide stronger connectivity and enhanced rigidity around the coordination center, and this property is reflected in higher stability of the resulting framework materials.<sup>25–27</sup>

$\beta$ -Diketonates are among the most studied ligands in the chemistry of metal complexes.<sup>28–30</sup> Despite this, only relatively simple  $\beta$ -diketonates have been exploited as building units in supramolecular design.<sup>31–41</sup> Tetraacet-

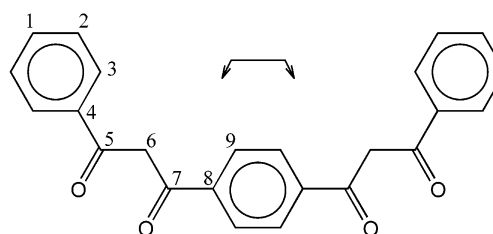


**Figure 1.**  $H_2L$ : structural formula, atom numbering scheme, and a schematic representation as a bar with two arrows showing two  $\beta$ -diketonate functions.

ylethane<sup>42</sup> is the simplest tetraketone with two separated  $\beta$ -diketonate functions, but only a few studies on the coordination species it forms have been reported.<sup>43–47</sup> Other studies on metal complexes with tri- and tetraketones are quite limited.<sup>48–51</sup> The present work introduces a new ligand with two separated  $\beta$ -diketonate functions (Figure 1). This ligand was expected to be capable of producing both polymeric and discrete complexes (Figure 2).

## Experimental Section

**Ligand ( $H_2L$ ) Synthesis.** The tetraketone, 1,4-bis(3-phenyl-1,3-propanedion)benzene (hereinafter  $H_2L$ ), was prepared in three steps. (i) The diacetylenic diketone  $Ph-C\equiv C-CO-Ph-CO-C\equiv C-Ph$  (first reported by Vereshchagin et al.<sup>52</sup>) was synthesized from phenylacetylene and dichloroanhydride of terephthalic acid by the method of catalytic acetylation.<sup>53</sup> (ii) Diaminodivinyl ketone  $Ph-C(NHPh)=CH-CO-Ph-CO-CH=C(NHPh)-Ph$  (first reported by Vereshchagin et al.<sup>54</sup>) was

\* To whom correspondence should be addressed. Tel: (613) 993-4406. Fax: (613) 998-7833. E-mail: Dmitriy.Soldatov@nrc.ca.

<sup>†</sup> National Research Council of Canada.

<sup>‡</sup> Institute of Inorganic Chemistry, Siberian Branch of the Russian Academy of Sciences.

<sup>§</sup> Institute of Chemical Kinetics and Combustion, Siberian Branch of the Russian Academy of Sciences.

Table 1. Single-Crystal X-ray Data Collection and Structure Analysis Details

compound	H <sub>2</sub> L, stable form	H <sub>2</sub> L, metastable form	[ZnPy <sub>2</sub> L] <sub>n</sub> * nPy	[Co <sub>3</sub> Py <sub>6</sub> L <sub>3</sub> ]* 4.84(CHCl <sub>3</sub> )	[Co <sub>3</sub> Py <sub>6</sub> L <sub>3</sub> ]* 4.11(CHCl <sub>3</sub> )	[Ni <sub>3</sub> Py <sub>6</sub> L <sub>3</sub> ]* 4.68(CHCl <sub>3</sub> )
refined guest:host ratio			1.00(1)	4.84(3)	4.11(5)	4.68(5)
empirical formula	C <sub>24</sub> H <sub>18</sub> O <sub>4</sub>	C <sub>24</sub> H <sub>18</sub> O <sub>4</sub>	C <sub>34</sub> H <sub>26</sub> O <sub>4</sub> N <sub>6</sub> Zn, (C <sub>5</sub> H <sub>5</sub> N)	C <sub>102</sub> H <sub>78</sub> Co <sub>3</sub> O <sub>12</sub> N <sub>6</sub> , 4.84(CHCl <sub>3</sub> )	C <sub>102</sub> H <sub>78</sub> Co <sub>3</sub> O <sub>12</sub> N <sub>6</sub> , 4.11(CHCl <sub>3</sub> )	C <sub>102</sub> H <sub>78</sub> O <sub>12</sub> N <sub>6</sub> Ni <sub>3</sub> , 4.68(CHCl <sub>3</sub> )
formula weight	370.4	370.4	671.0	2334.5	2245.5	2314.5
temperature of study (°C)	−100	−100	−100	−100	−100	−100
crystal system	monoclinic	monoclinic	monoclinic	trigonal	trigonal	trigonal
space group	<i>P</i> 2 <sub>1</sub> / <i>c</i>	<i>C</i> 2/ <i>c</i>	<i>C</i> 2/ <i>c</i>	<i>R</i> 3	<i>R</i> 3	<i>R</i> 3
unit cell dimensions						
<i>a</i> (Å)	10.161(2)	12.020(2)	20.609(5)	24.665(3)	24.613(3)	24.640(4)
<i>b</i> (Å)	7.453(1)	3.8803(6)	9.239(2)			
<i>c</i> (Å)	12.178(2)	38.285(6)	19.972(5)	30.702(4)	30.349(4)	30.549(5)
β (°)	103.79(1)	97.70(1)	120.28(1)			
<i>V</i> (Å <sup>3</sup> )	895.7(3)	1769.6(5)	3284(1)	16176(3)	15922(3)	16062(5)
<i>Z</i>	2	4	4	6	6	6
<i>D</i> <sub>calc</sub> (g/cm <sup>3</sup> )	1.373	1.390	1.357	1.438	1.405	1.436
μ (Mo Kα) (cm <sup>−1</sup> )	0.93	0.94	7.94	8.78	8.34	9.34
crystal color and shape	yellow prism	yellow sheet	yellow shapeless	red block	red block	green block
crystal sizes (mm)	0.4 0.2 0.2	0.6 0.4 0.01	0.1 0.1 0.1	0.4 0.3 0.1	0.3 0.3 0.3	0.1 0.1 0.1
goodness of fit on <i>F</i> <sup>2</sup>	1.062	1.113	0.847	0.984	1.017	0.871
final <i>R</i> 1, <i>wR</i> 2 ( <i>I</i> > 2σ( <i>I</i> ))	0.040, 0.120	0.073, 0.177	0.065, 0.104	0.057, 0.151	0.080, 0.202	0.058, 0.135
res. extrema (e/Å <sup>3</sup> )	−0.15, +0.37	−0.23, +0.35	−0.30, +0.63	−0.43, +0.75	−0.51, +1.11	−0.42, +0.76

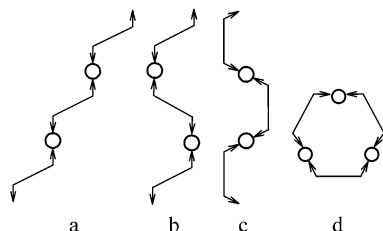


**Figure 2.** Possible modes of self-assembly of the title ligand (bar with two arrows) with metal centers (circles): (a,b) polymeric chains with the ligand in trans conformation; (c) polymeric chain with the ligand in cis conformation; (d) trinuclear complex with the ligand in cis conformation.

prepared from the diacetylenic diketone by the method of nucleophilic addition.<sup>55</sup> (iii) The final product was obtained as follows. The diaminodiviny ketone (10.36 g; 0.02 mol) was stirred at 80 °C in a mixture of aqueous HCl (15%, 20 mL) and dioxane (100 mL) for 5 h. After that, an excess of water was added and the precipitated yellow product was separated by filtration and recrystallized from tetrahydrofuran. The yield was 6 g (>80%); mp 195–198 °C. <sup>1</sup>H NMR (CDCl<sub>3</sub>): δ 6.94 (2H, enol C–H), 7.54 (4H, *m*-Ph), 7.61 (2H, *p*-Ph), 8.04 (4H, *o*-Ph), 8.11 (4H, phenylene), 16.83 (2H, enol O–H) ppm. Anal. (mass %) calcd for C<sub>24</sub>H<sub>18</sub>O<sub>4</sub> (370.4): C, 77.82; H, 4.90. Found: C, 77.70; H, 4.78.

**Ligand Polymorphs.** Two crystalline forms of the H<sub>2</sub>L were isolated. As the forms were distinct (as attested by solid state experimental characterization) but produced essentially the same solutions (as attested with <sup>1</sup>H NMR), they were thus confirmed as polymorphs.<sup>56</sup> A stable polymorph of H<sub>2</sub>L was obtained as prisms or blocks upon evaporation of chloroform, methylene chloride, and tetrahydrofuran solutions of the ligand. A metastable polymorph formed reproducibly as very thin sheets upon cooling of a warm acetone solution. The sheets while still in solution slowly converted into blocks of the stable polymorph. Evaporation of pyridine solutions produced a mixture of the two polymorphs. For characterization, see the Results and Discussion section.

**Metal Complexes.** These were isolated as single crystals. Zinc, cobalt, and nickel complexes were yellow, red, and green, respectively. Loss of guest solvent was observed in all cases. For single-crystal X-ray diffraction (XRD) experiments, the crystals were immediately cooled to −100 °C as soon as they were removed from the experimental conditions under which they were prepared.

**(a) [ZnPy<sub>2</sub>L]<sub>n</sub>\*nPy.** A warm solution of zinc acetate dihydrate (220 mg, 1 mmol) in pyridine (4 g) and a warm solution of H<sub>2</sub>L (185 mg, 0.5 mmol) in pyridine (7 g) were mixed, filtered, and left for slow evaporation. Shapeless crystals of up to 0.1 mm in size grew on the walls of the vial in 1 week.

**(b) [Co<sub>3</sub>Py<sub>6</sub>L<sub>3</sub>]\*xCHCl<sub>3</sub>.** The solution of cobalt(II) acetate tetrahydrate (13 mg, 0.05 mmol) in pyridine (0.1 g) and water (2 g) was layered over a solution of H<sub>2</sub>L (19 mg, 0.05 mmol) in chloroform (1.6 g). Red blocks of up to 1 mm in size grew near the interface (in the lower organic layer) in 1 week. Single-crystal XRD analysis performed on a “fresh” crystal indicated a total guest-to-host ratio of *x* = 4.84(3). Another crystal, exposed to air for 1 day, had *x* = 4.11(5). On further loss of guest, the same structure seems to be retained but the crystals become unsuitable for single-crystal XRD.

**(c) [Ni<sub>3</sub>Py<sub>6</sub>L<sub>3</sub>]\*xCHCl<sub>3</sub>.** The compound was prepared following the same procedure as for the cobalt compound. Refined *x* = 4.68(5).

**Single-Crystal XRD.** A Bruker SMART-1000 CCD X-ray diffractometer (Mo Kα radiation, λ = 0.71073 Å, graphite monochromator) was used to collect diffraction data. Full data sets were collected at −100 °C using the ω scan mode over the 2θ range of 2–58°. The coverage of the unique sets was over 99%. An empirical absorption correction SADABS<sup>57</sup> was applied. The final unit cell parameters were obtained using the entire data sets. Crystal data and experimental details of the low-temperature experiments are listed in Table 1 and in the Supporting Information.

The structures were solved (direct methods) and refined (difference Fourier synthesis) using the SHELXTL package.<sup>57</sup> The structural refinement was performed on *F*<sup>2</sup> and applied to all data with positive intensities. Nonhydrogen atoms were refined anisotropically. The guest pyridine molecule was refined as benzene as the nitrogen atom was not localized. To avoid unreasonable distortions due to disorder, all guest chloroform molecules were refined using rigid-body model constraints on molecular geometry and thermal parameters. Site occupancy factors were refined where significant deviations from the ideal stoichiometry were observed; the ideal and actual guest-to-host ratios are given in Table 1. Further experimental details, as well as full lists of derived results, are given in the Supporting Information.

Most of the crystals studied in this work were of poor quality. The largest residual maxima (>0.5 e/Å<sup>3</sup>) on the final difference maps were observed in the vicinity of metal atoms and arose from inadequate absorption corrections rather than from unresolved atoms.

For the H<sub>2</sub>L polymorphs, the room temperature unit cell dimensions were also measured.<sup>58</sup> To accomplish this, several dozens of reflections were found randomly using 120 or more frame  $\omega$  scans, 0.3° wide, starting at three different  $\phi$  positions.

**Powder XRD.** Phase analyses were carried out on a Rigaku Geigerflex diffractometer with Co K $\alpha$  radiation ( $\lambda = 1.7902$  Å) in the 5–30° 2 $\theta$  range, with a 0.02° step scan, 1 s per step. For calculated powder patterns, the low-temperature single-crystal analysis results (Table 1) were used with unit cell dimensions determined at room temperature.<sup>58</sup>

**NMR Spectroscopy.** <sup>1</sup>H and <sup>13</sup>C NMR spectra were obtained on a Bruker DRX-400 instrument for 0.05 M solutions of the H<sub>2</sub>L polymorphs and for 0.1 M solution of dibenzoylmethane in deuterated chloroform. Integration of bands was performed with the XWIN NMR 2.0 program package.

Solid state <sup>13</sup>C cross-polarization/magic angle spinning (CP/MAS) NMR spectra were obtained at 75.43 MHz at room temperature on a Bruker AMX300 spectrometer equipped with a Doty Scientific 5 mm CP/MAS probe. A standard CP pulse program was used with fixed amplitude <sup>1</sup>H decoupling during signal acquisition. <sup>1</sup>H 90° pulse lengths were 3  $\mu$ s, CP times were 3 ms, recycle times were 6 s, and the spinning rate was 5.5 kHz. Chemical shifts were measured relative to external solid hexamethylbenzene and then corrected to the TMS scale. Dipolar dephasing (nonquaternary suppression) spectra were also obtained with a 40  $\mu$ s interruption of <sup>1</sup>H decoupling between cross-polarization and data acquisition.

**Calculations.** Channel profiles were calculated by finding the diameter of the largest possible inscribed sphere that is in van der Waals contact with the channel walls as the center of the sphere moves along the channel axis.<sup>59</sup> The coordinates of the sphere were (0,0,*Z*), where *Z* was a variable expressed as a fraction of the *c* crystallographic translation. Either all guest species or only those residing near the 3-fold axis were removed from the atom lists in these calculations. All numerical data used in the calculations are listed in the Supporting Information. The following system of van der Waals radii was applied everywhere:<sup>60,61</sup> C, 1.71; H, 1.16; Co, 1.50; Cl, 1.90; N, 1.52; Ni, 1.63; O, 1.29 Å.

## Results and Discussion

### H<sub>2</sub>L: Molecular Structure and Polymorphism.

The title tetraketone bears two  $\beta$ -diketone functions separated by a phenylene ring (Figure 1). The  $\beta$ -diketone fragments are presumably planar, not only upon chelating metal centers but even in the free ligand in solution (<sup>1</sup>H NMR data confirm that 100% of the ligand exists in the enol form). Therefore, the ligand is a system of five planar fragments connected by single C–C bonds. However, the conformational freedom of the ligand is restricted to two preferable geometries, probably because the  $\pi$ -systems of all of the fragments can interact. Both conformations are planar with 180 and 0° dihedral angles between  $\beta$ -diketone functions for trans and cis isomers, respectively.

The ligand was isolated and studied in two polymorphic forms (Table 1). The molecular structure and geometry are very similar in both polymorphs, with the molecule in the enol form in a centrosymmetric trans conformation, and the whole unit displays a tendency to be planar (Figure 3).

The enol hydroxy group takes part in the formation of an intramolecular hydrogen bond to the other oxygen atom of the  $\beta$ -diketone function (the O...O distance ranges within 2.44–2.46 Å and the O–H...O angle within 148–150°). The hydrogen atom is equally disordered between two positions associated with two keto-oxygens. The CC distances in the enol ring (1.40 Å) are equal within experimental error and are indicative of

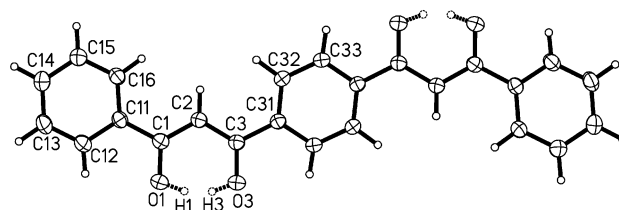


**Figure 3.** Molecule of the free H<sub>2</sub>L ligand as found in its stable polymorph. H1 and H3 are half occupied and represent two positions of a disordered hydrogen.

50% double bond character. The CO bond lengths (1.29–1.30 Å) are intermediate between those of typical C=O (1.23 Å) and C–O (1.43 Å) bonds. All of these geometric considerations suggest interconversion between the two enol forms.

The conformational features differ only slightly in the two polymorphs. In the stable polymorph, the enol ring and terminal phenyl are almost coplanar, with a dihedral angle between their planes of 0.4°, and the central phenylene ring is rotated by 13.2° from the plane of the enol ring. In the metastable polymorph, the enol ring and terminal phenyl form a dihedral angle of 7.1° while the central phenylene ring is rotated by 1.2° from the plane of the enol ring. This tendency to coplanarity and other geometric features was previously observed in dibenzoylmethane,<sup>62–65</sup> its derivatives,<sup>66,67</sup> and its metal complexes.<sup>33–35,68</sup>

The first observation from the solid state <sup>13</sup>C CP/MAS NMR spectra, Figure 4, is that they show a distinction between the two polymorphs, with different shifts for most of the lines. Even without the X-ray structural information, it is clear that these are two different phases. Assignments, together with those for the ligand in CDCl<sub>3</sub> solution, are given in Table 2 (see Figure 1 for the numbering scheme).

Spectra obtained with nonquaternary suppression (dipolar dephasing) help in making the assignments since they only show those carbons that are not attached to <sup>1</sup>H. These also clearly show that the C1 and C4 resonances are practically on top of each other in the spectra of the stable polymorph but 4.9 ppm apart in the metastable polymorph. Likewise, the CO resonances of C5 (adjacent to phenyl) and C7 (adjacent to phenylene) are well-resolved for the metastable polymorph (2.3 ppm) but not quite resolved for the stable form (which shows a flat-topped peak). The multiplicities of the spectra are consistent with the molecules being centrosymmetric and with an asymmetric unit containing half of the molecule, in agreement with the X-ray structural analysis. The differences in crystal packing of the two polymorphs create different intramolecular torsional angles and intermolecular contacts. Hence, different combinations of several environmental factors influence the chemical shifts of equivalent atoms in the two forms, resulting in the small differences in the <sup>13</sup>C NMR shifts.

The crystal packing is shown in Figure 5. Flat molecules of ~22 Å in length and ~8 Å in width are offset, stacked in layers that allow favorable  $\pi$ – $\sigma$  interactions.<sup>69</sup> The distance between the least-squares planes of the molecules (3.54 and 3.53 Å in the stable and metastable forms, respectively) is defined by the



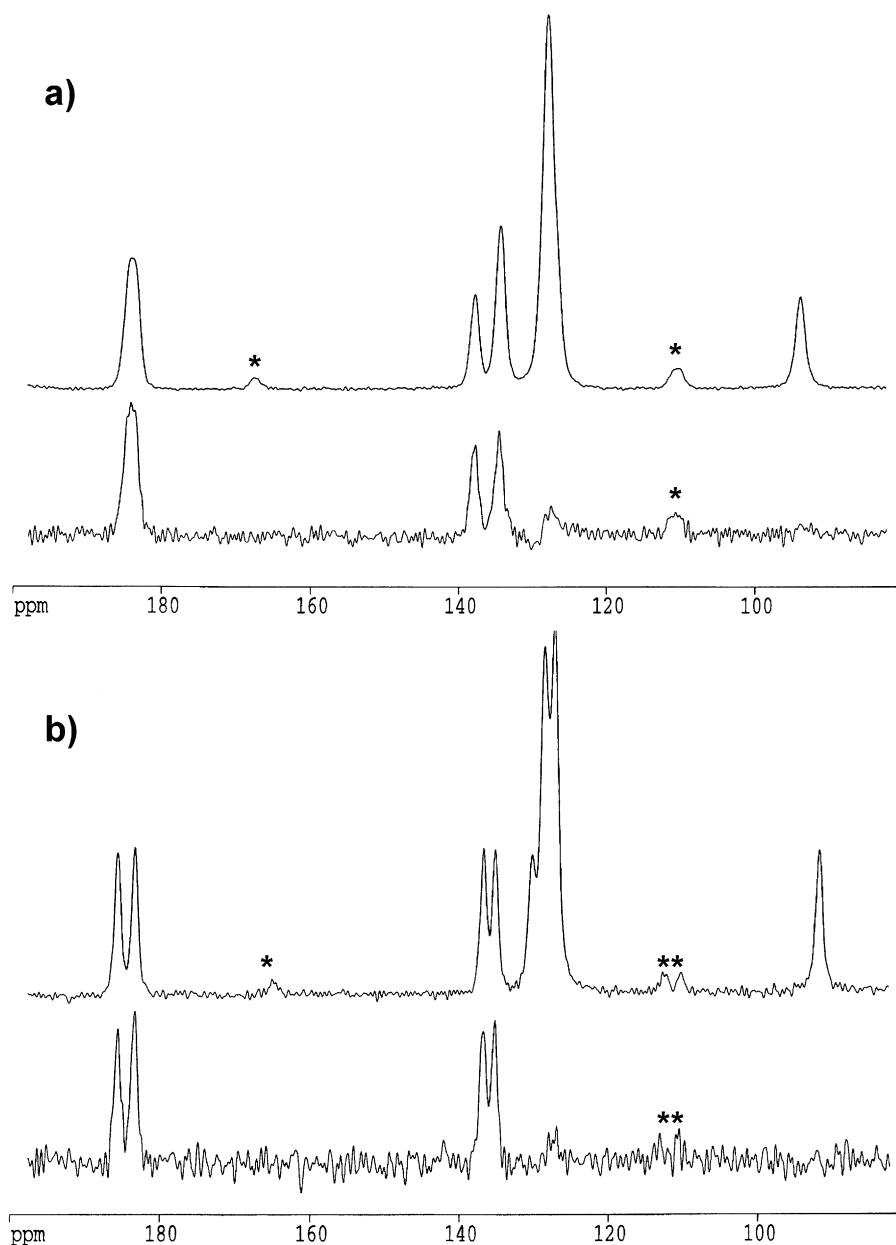


**Figure 4.**  $^{13}\text{C}$  CP/MAS NMR spectra of the stable (a) and metastable (b) polymorphs of  $\text{H}_2\text{L}$ . The lower spectrum in each case shows the quaternary carbon resonances (dipolar dephased spectrum). Spinning sidebands are indicated by asterisks (\*).

van der Waals radius of the carbon atom and provides effective intermolecular contacts.

Differences in the packing are reflected in the growth of the crystals. Crystals of the stable form are compact while the metastable form grows as very thin sheets. Powder XRD experiments performed on both ground and intact crystals showed that the faces of the sheets are (001) planes. In other words, the fast growth of the metastable form occurs in the *a* and *b* directions. In the *a* direction, the crystal growth is favored by intermolecular dipole–dipole interactions between  $\beta$ -diketone functions aligned along this direction, and in the *b* direction, the growth is presumably driven by the stacking mechanism. In the *c* direction, the molecules contact only the ribs of terminal phenyls, which makes the growth slower.

The metastable form has a unit cell with one very short (less than 4 Å) and one very long (greater than

**Table 2.**  $^{13}\text{C}$  NMR Chemical Shifts (ppm) and Assignments of  $\text{H}_2\text{L}$  (for Numbering Scheme, See Figure 1)

atom no. (multiplicity)	description <sup>a</sup>	solution in $\text{CDCl}_3$ <sup>b</sup>	stable phase <sup>b</sup>	metastable phase <sup>b</sup>
6(1)	C–H	94.2 (1)	94.0 (1)	91.9 (1)
3(2), 9(2)	Ph–H, Ph'–H	127.7 (2), 127.8 (2)	128.2 (6)	127.2, 128.5 (6)
2(2)	Ph–H	129.2 (2)		
1(1)	Ph–H	133.2 (1)	134.4 <sup>c</sup> (1)	130.3 (1)
4(1) <sup>d</sup>	Ph–q	135.9 (1)	134.6 <sup>c</sup> (1) q	135.2 (1) q
8(1) <sup>d</sup>	Ph'–q	139.1 (1)	137.9 (1) q	136.8 (1) q
5(1), 7(1)	CO	183.9 (1), 187.5 (1)	184.3 (2) q	183.4 (1) q, 185.7 (1) q

<sup>a</sup> Ph, phenyl; Ph', phenylene; q, quaternary. <sup>b</sup> Relative intensities in brackets. <sup>c</sup> These two strongly overlapping peaks are distinguished by the nonquaternary suppression experiment. <sup>d</sup> The C4 and C8 distinction is tentative, based on the assigned shifts of the ipso-C (equivalent to C4) in dibenzoylmethane at 135.6 and 132.7 ppm (for two crystallographically inequivalent ipso-C in the solid) and 134.3 ppm in solution.<sup>68</sup>

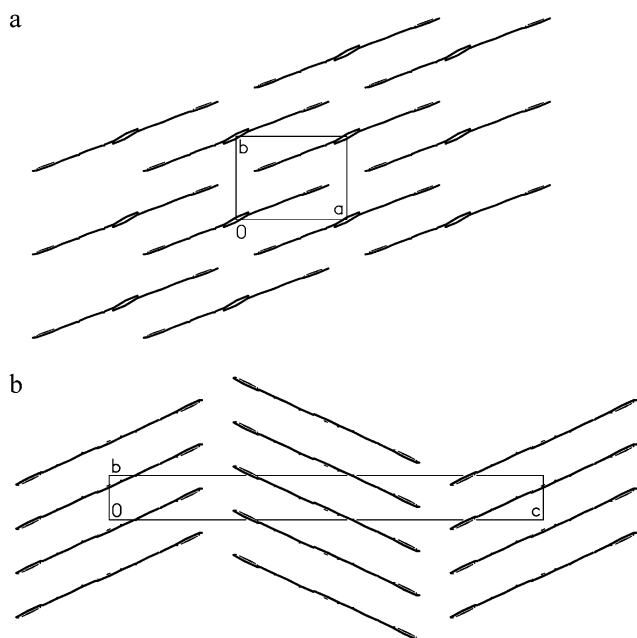


**Figure 5.** Packing diagrams of the two polymorphic modifications of free H<sub>2</sub>L ligand. (a) Stable polymorph, projection along *c*, half of unit cell content. (b) Metastable polymorph, projection along *a*, half of unit cell content.

38 Å) parameter. A search for other crystal structures with similar dimensions, which were solved to atomic coordinates, performed on the Cambridge Structural Database,<sup>70</sup> revealed only 15 entries (out of 272 066). All contained aromatics, and most showed planarity and presumably an expansive delocalization of electron density over conjugated<sup>71,72</sup> or condensed<sup>73,74</sup> aromatic fragments.

**Coordination Compounds.** As expected, the ligand readily forms coordination compounds. However, the ability to chelate two metal centers simultaneously presented difficulties for the preparation of pure monophase products. A series of experiments with a variety of conditions resulted in only a few cases where single crystals suitable for characterization were obtained. The results of single-crystal XRD studies on the samples illustrate that two modes of assembly with metal cations (Figure 6) resulted from the conformational isomerism of the ligand.

The [ZnPy<sub>2</sub>L]<sub>*n*</sub>·*n*Py compound is a one-dimensional (1D) coordination polymer (type a in Figure 2). The ligand adopts a trans conformation and chelates two zinc atoms, bridging them at a distance of 11.3 Å (Figure 6). The coordination environment of each zinc atom, shown in Figure 7, is a slightly distorted octahedron formed by two chelate rings in the equatorial plane (Zn–O distances 2.05–2.06 Å) and two axially coordinated pyridines (Zn–N distance 2.18 Å). The coordination angles are ideal to within 1°.

In this compound, the ligand fragments are not coplanar. The terminal phenyl and central phenylene form, with the chelate ring, dihedral angles of 15.0 and 31.3°, respectively. These conformational features may be attributed to the packing requirements of the branched polymeric chains into a three-dimensional (3D) architecture. Another factor facilitating packing is the presence of additional pyridine included as guest.

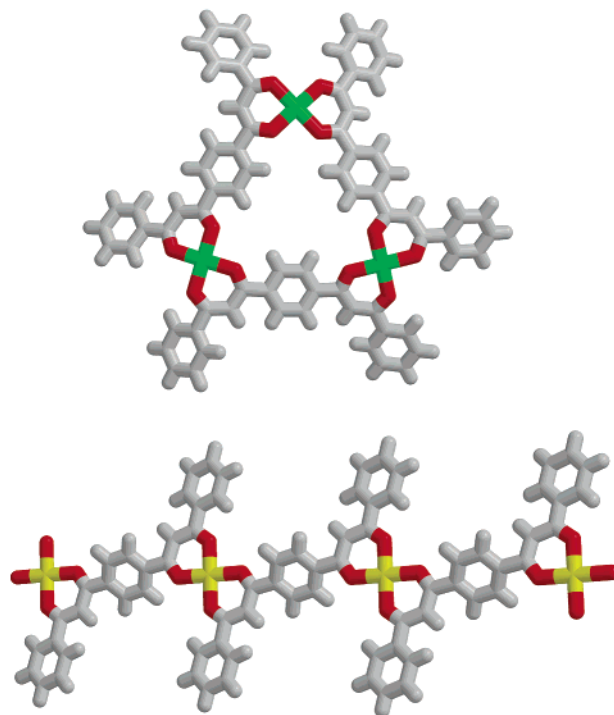


**Figure 6.** Two types of assembly of the title ligand with metal cations as found in the present study: the triangular complex with Ni(II) or Co(II) and the polymeric complex with Zn(II). For clarity, pyridine ligands are omitted.

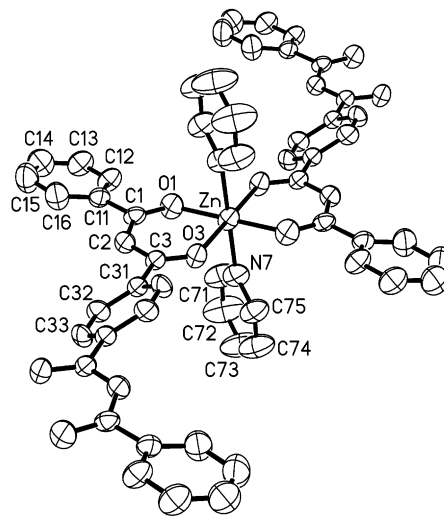


**Figure 7.** Molecular structure of the host complex in the [ZnPy<sub>2</sub>L]<sub>*n*</sub>·*n*Py compound: fragment of the polymeric chain showing octahedral coordination environment of Zn(II). Bond lengths: Zn–O1, 2.045(3) Å; Zn–O3, 2.058(2) Å; Zn–N7, 2.175(3) Å. H-atoms are omitted.

The crystal packing is shown in Figure 8. At *z* = 0, the host polymeric chains run diagonally in the (*ab*) plane. At *z* = 0.5, the chains run along another diagonal. Guest molecules are located between these two layers, at *z* = 0.25 and *z* = 0.75.

The compounds isolated from preparations with cobalt(II) and nickel(II) comprise discrete trimeric rather than polymeric complex species, as shown in Figure 6 (type d in Figure 2). Three crystals showed the same basic architecture with ideal formula [M<sub>3</sub>Py<sub>6</sub>L<sub>3</sub>]\*5-(CHCl<sub>3</sub>) (Table 1). Here, only the cobalt structure, for

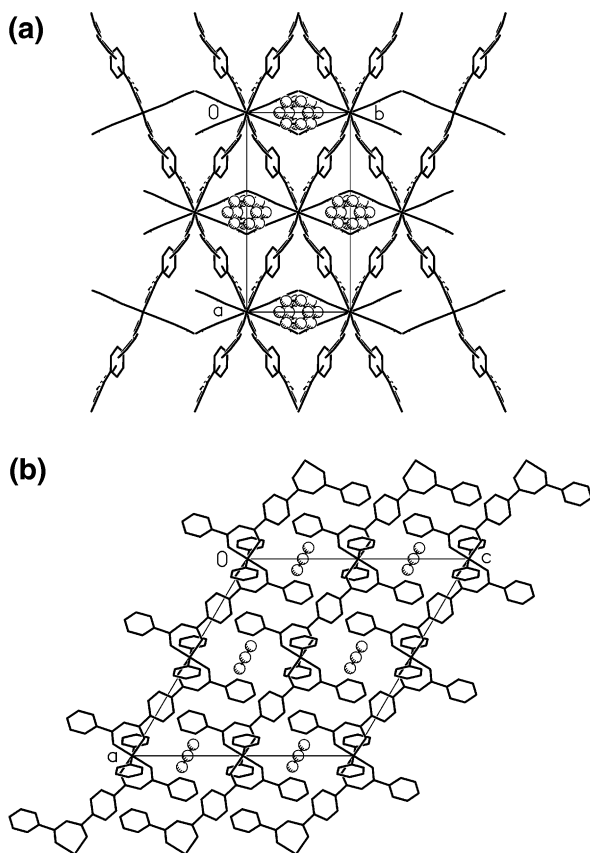


**Figure 8.** Crystal structure of the  $[\text{ZnPy}_2\text{L}]_n \cdot n\text{Py}$  compound. (a) Unit cell contents down  $c$ -axis. (b) The same fragment viewed down  $b$ -axis. Guest molecules are enlarged for clarity.

which two crystals with different guest content were studied, will be described in detail. The nickel compound is very similar and serves to demonstrate that the basic architecture can be modified by substituting different metal centers.

The  $[\text{Co}_3\text{Py}_6\text{L}_3] \cdot 4.84(\text{CHCl}_3)$  compound has a trigonal structure, space group  $R\bar{3}$ . The ligand adopts a cis conformation and chelates two cobalt atoms bridging them at a distance of 10.7 Å. Three ligands chelate three cobalt centers to form a triangular trinuclear complex (Figure 9). The coordination environment of each cobalt atom is a distorted octahedron, formed by two chelate rings in the equatorial plane (Co–O distances 2.02–2.04 Å) and two axially coordinated pyridines (Co–N distance 2.17–2.18 Å). The dihedral angle of 31.5° between two chelate fragments adjacent to the cobalt center is quite large. The coordination angles deviate from ideal by up to 5°.

The ligand conformation deviates from planar to satisfy connectivity and packing requirements (Figure 9). The central phenylene ring forms angles of 4.0 and 16.0° with respect to the chelate fragments (O1, C1–C3, O3) and (O4, C4–C6, O6), respectively, and the chelate fragments form angles of 33.4 and 5.0° with the terminal phenyl rings (C11–C16) and (C61–C66), respectively.

The triangular complexes are stacked along the  $-3$  axis forming a channel (Figure 10). Two triangular units, related by the  $-3$  symmetry element and located at  $z = 0.31$  and  $z = 0.69$ , are separated by 11.9 Å from each other, and the distance to the next unit is 18.5 Å.

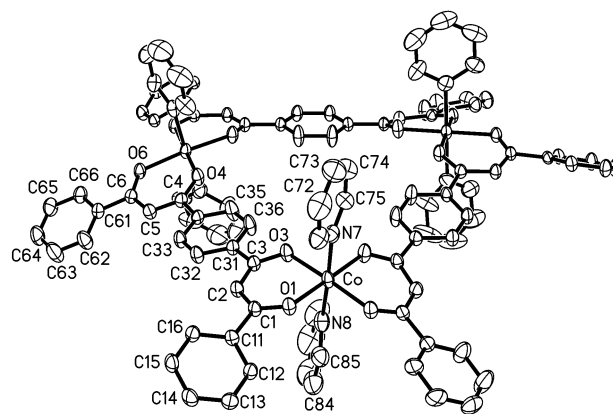


**Figure 9.** Molecular structure of the host trinuclear complex in the  $[\text{Co}_3\text{Py}_6\text{L}_3] \cdot 4.84(\text{CHCl}_3)$  compound. Co(II) is in a distorted octahedral environment (coordination angles deviate from ideal by up to 5°). Bond lengths: Co–O1, 2.038(2) Å; Co–O3, 2.036(2) Å; Co–O4', 2.021(2) Å; Co–O6', 2.035(2) Å; Co–N7, 2.167(2) Å; Co–N8, 2.183(3) Å. H-atoms are omitted.

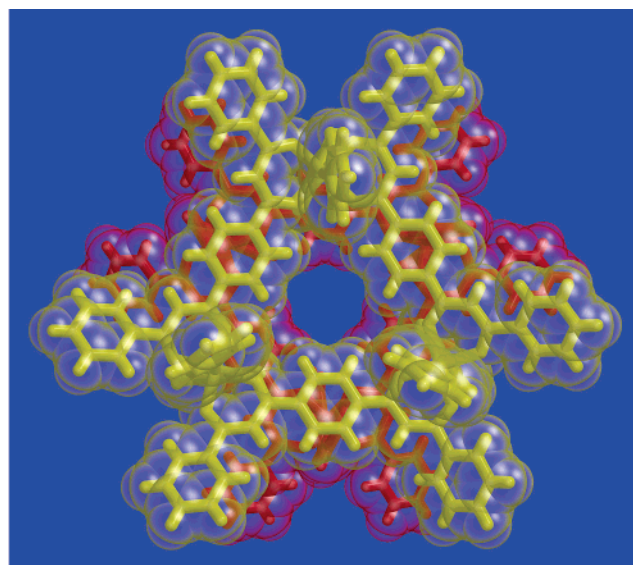


**Figure 10.** Packing of triangular complexes along  $z$  forming a channel in  $[\text{Co}_3\text{Py}_6\text{L}_3] \cdot 4.84(\text{CHCl}_3)$ . The surroundings of the channel are shown in van der Waals dimensions.

The walls of the channel are completed by phenyls from neighboring triangular complexes.

The profile of the channel is shown in Figure 11. The diameter of the channel changes from 0.8 to 5.7 Å. The narrowest restriction at  $z = 0.07$  is formed by three terminal phenyls from three units associated with parallel channels. These phenyls act as locks, as their rotation opens side chambers capable of circumscribing a sphere of 4 Å in diameter, which makes it possible for guest molecules to diffuse through the channels. Another restriction at the level  $z = 0.31$ , 3.7 Å in diameter, corresponds to the hole in the triangular complex. Rotation of the central phenylene rings can widen this diameter to 6.3 Å. There are no evident connections between the neighboring channels, whose centers are separated by 14.2 Å. However, taking into account van der Waals packing, the low density of the structure and the presence of a great number of rotating phenyl, phenylene, and pyridine rings, diffusion of the guest between the channels cannot be excluded.

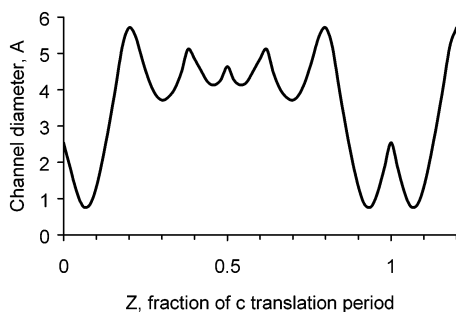


**Figure 11.** Channel diameter profile for the  $[\text{Co}_3\text{Py}_6\text{L}_3] \cdot 4.84\text{-(CHCl}_3\text{)}$  structure. The profile is outlined as the diameter of the largest possible inscribed sphere that is in van der Waals contact with the host atoms as the center of the sphere moves along the  $z$ -direction. The profile shows restrictions for movement of the guest molecules directly along the channel but does not account for their diffusion through side niches.

In fact, there is experimental evidence that the guest is able to diffuse through the channels. After recovering crystals from the crystallization media, they show loss of guest chloroform. The process demonstrates “organic zeolite” behavior,<sup>75,76</sup> where the crystal framework is preserved as the guest leaves the structure. Visual changes associated with loss of the guest were (i) cracking of the crystals due to volume contraction of the host matrix and (ii) retention of transparency of the crystals, rather than the disintegration into a powdery material, which would be expected upon formation of a new, dense phase of the host.

Further evidence of the organic zeolite behavior of the crystals of  $[\text{Co}_3\text{Py}_6\text{L}_3] \cdot x(\text{CHCl}_3)$  comes from direct single-crystal XRD analysis of two crystals, which exhibited the same structure but differed in the content of guest ( $x$ ). The first crystal, exposed to air for just a few minutes, had  $x = 4.84(3)$ , while the second, deliberately exposed to air for 1 day, had  $x = 4.11(5)$ . Furthermore, it was visually obvious that the structure is retained in the course of further loss of guest. Unfortunately, considerable cracking made the crystals unsuitable for single-crystal structural analysis. One of the crystals exposed to air for 3 days had a unit cell volume of 15794(4) Å<sup>3</sup>, indicating further contraction of the structure (as compared with 16176(3) and 15922(3) Å<sup>3</sup> for crystals with  $x = 4.84(3)$  and  $x = 4.11(5)$ , respectively, Table 1).

There are three crystallographically distinct guest sites in  $[\text{Co}_3\text{Py}_6\text{L}_3] \cdot x(\text{CHCl}_3)$ . The first is a general position in the side niches of the channel at  $z = 0.2$  and  $0.8$ . A second and third are inside the channel at  $z = 0.2$  and  $0.4$ , respectively. All guest molecules are disordered over 2–4 orientations, not counting the disordering over the  $-3$  axis. A projection of the structure on the  $c$ -axis showing the packing and the location of the channels and guest molecules is given in Figure 12.

The comparison of two  $[\text{Co}_3\text{Py}_6\text{L}_3] \cdot x(\text{CHCl}_3)$  crystals with  $x = 4.84$  and  $4.11$  shows that the structure keeps the same motif but experiences a significant contraction as the guest leaves the channels. The unit cell volume contracts by 1.6% as a result of the 15% guest removal. Guest occupancies are close to 100% for every position in the initial sample, whereas in the depleted sample this had reduced to 84(1)% in the niche sites and 96(4) and 63(2)% in the channel sites at  $z = 0.2$  and  $0.4$ ,

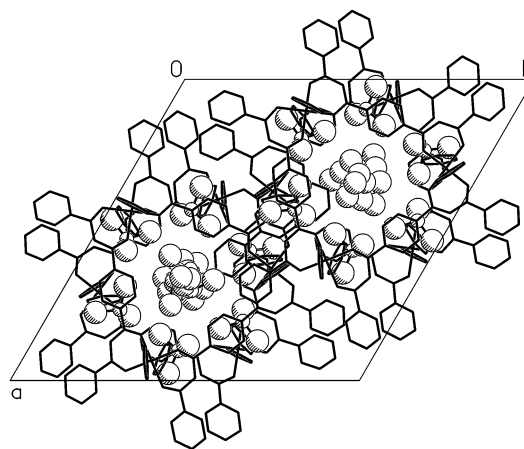


**Figure 12.** Packing diagram of the  $[\text{Co}_3\text{Py}_6\text{L}_3] \cdot 4.84(\text{CHCl}_3)$  compound. Projection of the structure along the  $c$ -axis. For clarity, guest molecules are enlarged, and only their major orientations are shown.

respectively. An analysis of the channel profile shows that the channel experiences widening at  $z = 0.2$  and narrowing at  $z = 0.4$  upon contraction, which helps to explain the disproportionate guest distribution between the sites.

The design of novel materials that exhibit zeolite-like behavior is of considerable interest. One approach to such design is to create highly robust metal–organic frameworks that retain their microporosity after guest removal because their covalently bonded 3D architectures have significant kinetic stability.<sup>25–27,77,78</sup> Another approach is to create more flexible structures,<sup>79–86</sup> which can retain their architectures while changing and contracting to some extent upon guest removal. These flexible architectures, also referred to as “dynamic” frameworks,<sup>87</sup> are especially promising for development of functional and smart materials, which sense and respond to external changes such as the presence of certain absorbates.<sup>17,88,89</sup>

The  $[\text{M}_3\text{Py}_6\text{L}_3] \cdot x(\text{CHCl}_3)$  materials discussed here exemplify one way to create such flexible architectures. The utilization, in the design of porous solids, of nanoscale macrocycles or “molecular boxes”, which have an intrinsic predisposition to form cavity space and which preclude interpenetration, has been reported.<sup>47,90–96</sup> In this work, we have demonstrated how a structure, designed in such a way, reveals flexibility in adjusting to guest removal while retaining its basic architecture.

**Acknowledgment.** We thank Stephen Lang, Md. Badruz Zaman, Pierre Desjardins, and Philip Brown for their helpful comments on the work. D.V.S. is thankful to E. V. Grachev (Institute of Inorganic Chemistry, Novosibirsk) for the CLAT program package.

**Supporting Information Available:** Figures comparing experimental and theoretical diffractograms for two polymorphic modifications of  $\text{H}_2\text{L}$ . Calculated channel profiles for  $[\text{M}_3\text{Py}_6\text{L}_3] \cdot x(\text{CHCl}_3)$  compounds. Tables of crystal data and details of single-crystal XRD experiments, bond lengths and angles, hydrogen-bonding parameters, anisotropic displacement parameters, and hydrogen atom coordinates for the six compounds studied (see Table 1 and ref 58) as well as the crystallographic data in CIF format. This material is available free of charge via the Internet at <http://pubs.acs.org>.



## References

- (1) Comprehensive Supramolecular Chemistry. In *Solid-State Supramolecular Chemistry: Crystal Engineering*; MacNicol, D. D., Toda, F., Bishop, R., Eds.; Pergamon: Oxford, 1996; Vol. 6.
- (2) Hanan, G. S.; Schubert, U. S.; Volkmer, D.; Rivi re, E.; Lehn, J.-M.; Kyritsakas, N.; Fisher, J. *Can. J. Chem.* **1997**, *75*, 169–182.
- (3) Shimizu, G. K. H.; Enright, G. D.; Ratcliffe, C. I.; Ripmeester, J. A.; Wayner, D. D. M. *Angew. Chem., Int. Ed. Engl.* **1998**, *37*, 1407–1409.
- (4) Champness, N. R.; Khlobystov, A. N.; Majuga, A. G.; Schr der, M.; Zyk, N. V. *Tetrahedron Lett.* **1999**, *40*, 5413–5416.
- (5) Fedin, V. P.; Kalinina, I. V.; Samsonenko, D. G.; Mironov, Y. V.; Sokolov, M. N.; Tkachev, S. V.; Virovets, A. V.; Podbereskaya, N. V.; Elsegood, M. R. J.; Clegg, W.; Sykes, A. G. *Inorg. Chem.* **1999**, *38*, 1956–1965.
- (6) Mironov, Y. V.; Virovets, A. V.; Naumov, N. G.; Ikorskii, V. N.; Fedorov, V. E. *Chem. Eur. J.* **2000**, *6*, 1361–1365.
- (7) Imamura, T.; Fukushima, K. *Coord. Chem. Rev.* **2000**, *198*, 133–156.
- (8) Baxter, P. N. W. *J. Org. Chem.* **2000**, *65*, 1257–1272.
- (9) Aaker y, C. B.; Beatty, A. M.; Leinen, D. S. *Cryst. Growth Des.* **2001**, *1*, 47–52.
- (10) Gryko, D. T. *Eur. J. Org. Chem.* **2002**, 1735–1743.
- (11) Zaman, M. B.; Smith, M. D.; Ciurtin, D. M.; zur Loye, H.-C. *Inorg. Chem.* **2002**, *41*, 4895–4903.
- (12) Dong, Y.-B.; Ma, J.-P.; Huang, R.-Q.; Smith, M. D.; zur Loye, H.-C. *Inorg. Chem.* **2003**, *42*, 294–300.
- (13) Keegan, J.; Kruger, P. E.; Nieuwenhuyzen, M.; Martin, N. *Cryst. Growth Des.* **2002**, *2*, 329–332.
- (14) Bosch, E.; Barnes, C. L. *Inorg. Chem.* **2001**, *40*, 3097–3100.
- (15) Bosch, E.; Schultheiss, N.; Rath, N.; Bond, M. *Cryst. Growth Des.* **2003**, *3*, 263–266.
- (16) Soldatov, D. V.; Ripmeester, J. A. *Stud. Surf. Sci. Catal.* **2002**, *141*, 353–362.
- (17) Nossor, A. V.; Soldatov, D. V.; Ripmeester, J. A. *J. Am. Chem. Soc.* **2001**, *123*, 3563–3568.
- (18) Halder, G. J.; Kepert, C. J.; Moubaraki, B.; Murray, K. S.; Cashion, J. D. *Science* **2002**, *298*, 1762–1765.
- (19) Fehlhammer, W. P.; Fritz, M. *Chem. Rev.* **1993**, *93*, 1243–1280.
- (20) Iwamoto, T. *J. Inclusion Phenom.* **1996**, *24*, 61–132.
- (21) Iwamoto, T. In *Comprehensive Supramolecular Chemistry*; MacNicol, D. D., Toda, F., Bishop, R., Eds.; Pergamon: Oxford, 1996; Vol. 6, Chapter 19, pp 643–690.
- (22) Dunbar, K. R.; Heintz, R. A. *Prog. Inorg. Chem.* **1997**, *45*, 283–391.
- (23) Zaworotko, M. J. *Chem. Commun.* **2001**, 1–9.
- (24) Moulton, B.; Zaworotko, M. J. *Chem. Rev.* **2001**, *101*, 1629–1658.
- (25) Yaghi, O. M.; Davis, C. E.; Li, G.; Li, H. *J. Am. Chem. Soc.* **1997**, *119*, 2861–2868.
- (26) Kristiansson, O.; Terenius, L.-E. *J. Chem. Soc., Dalton Trans.* **2001**, 1415–1420.
- (27) Eddaoudi, M.; Kim, J.; Rosi, N.; Vodak, D.; Wachter, J.; O’Keeffe, M.; Yaghi, O. M. *Science* **2002**, *295*, 469–472.
- (28) Fackler, J. P. *Prog. Inorg. Chem.* **1966**, *7*, 361–425.
- (29) Lingafelter, E. C. *Coord. Chem. Rev.* **1966**, *1*, 151–155.
- (30) Joshi, K. C.; Pathak, V. N. *Coord. Chem. Rev.* **1977**, *22*, 37–122.
- (31) Steinbach, J. F.; Burns, J. H. *J. Am. Chem. Soc.* **1958**, *80*, 1839–1841.
- (32) Ueda, T.; Eguchi, T.; Nakamura, N.; Wasylishen, R. E. *J. Phys. Chem. B* **2003**, *107*, 180–185.
- (33) Soldatov, D. V.; Ripmeester, J. A. *Chem. Eur. J.* **2001**, *7*, 2979–2994.
- (34) Soldatov, D. V.; Enright, G. D.; Ratcliffe, C. I.; Henegouwen, A. T.; Ripmeester, J. A. *Chem. Mater.* **2001**, *13*, 4322–4334.
- (35) Soldatov, D. V.; Enright, G. D.; Ripmeester, J. A. *Chem. Mater.* **2002**, *14*, 348–356.
- (36) Gromilov, S. A.; Baydina, I. A.; Zharkova, G. I. *J. Struct. Chem.* **1997**, *38*, 792–798; in Russian version, 946–953.
- (37) Soldatov, D. V.; Ripmeester, J. A. *Chem. Mater.* **2000**, *12*, 1827–1839.
- (38) Angelova, O.; Macicek, J.; Atanasov, M.; Petrov, G. *Inorg. Chem.* **1991**, *30*, 1943–1949.
- (39) Burdukov, A. B.; Guschin, D. A.; Pervukhina, N. V.; Ikorskii, V. N.; Shvedenkov, Yu. G.; Reznikov, V. A.; Ovcharenko, V. I. *Cryst. Eng.* **1999**, *2*, 265–279.
- (40) Caneschi, A.; Cornia, A.; Fabretti, A. C.; Gatteschi, D. *Angew. Chem., Int. Ed.* **1999**, *38*, 1295–1297.
- (41) Griesar, K.; Haase, W.; Svoboda, I.; Fuess, H. *Inorg. Chim. Acta* **1999**, *287*, 181–185.
- (42) Charles, R. G. In *Organic Syntheses*; Wiley: New York, 1963; Coll. Vol. 4, pp 869–871.
- (43) Lim, Y. Y.; Chen, W.; Tan, L. L.; You, X. Z.; Yao, T. M. *Polyhedron* **1994**, *13*, 2861–2866.
- (44) Kambayashi, H.; Yuzurihara, J.; Masuda, Y.; Nakagawa, H.; Linert, W.; Fukuda, Y. *Z. Naturforsch.* **1995**, *50b*, 536–544.
- (45) Kobayashi, Y.; Nagao, N.; Okeya, S.; Fukuda, Y. *Chem. Lett.* **1996**, 663–664.
- (46) Zhang, Y.; Wang, S.; Enright, G. D.; Breeze, S. R. *J. Am. Chem. Soc.* **1998**, *120*, 9398–9399.
- (47) Zhang, Y.; Breeze, S. R.; Wang, S.; Greedan, J. E.; Raju, N. P.; Li, L. *Can. J. Chem.* **1999**, *77*, 1424–1435.
- (48) Guthrie, J. W.; Lintvedt, R. L.; Glick, M. D. *Inorg. Chem.* **1980**, *19*, 2949–2956.
- (49) Casabo, J.; Colomer, J.; Escriche, L.; Teixidor, F.; Molins, E.; Miravittles, C. *Inorg. Chim. Acta* **1990**, *178*, 221–226.
- (50) Maverick, A. W.; Buckingham, S. C.; Yao, Q.; Bradbury, J. R.; Stanley, G. G. *J. Am. Chem. Soc.* **1986**, *108*, 7430–7431.
- (51) Saalfrank, R. W.; Seitz, V.; Caulder, D. L.; Raymond, K. N.; Teichert, M.; Stalke, D. *Eur. J. Inorg. Chem.* **1998**, 1313–1317.
- (52) Vereshchagin, L. I.; Kirillova, L. P.; Demina, S. I. *Russ. J. Org. Chem.* **1973**, *9* (2), 300–303 (*Zh. Org. Khim.* **1973**, *9* (2), 300–303, Russian).
- (53) Shergina, S. I.; Sokolov, I. E.; Zanina, A. S.; Kotlyarevskii, I. L. *Russ. Chem. Bull.* **1984**, *3*, 639–641 (*Izv. Akad. Nauk SSSR, Ser. Khim.* **1984**, *3*, 689–691, Russian).
- (54) Vereshchagin, L. I.; Kirillova, L. P.; Buzilova, S. R.; Bol’shedvorskaya, R. L.; Chernysheva, G. V. *Russ. J. Org. Chem.* **1975**, *11* (3), 527–532 (*Zh. Org. Khim.* **1975**, *11* (3), 531–537, Russian).
- (55) Sokolov, I. E.; Shergina, S. I.; Zanina, A. S. *Izv. Akad. Nauk SSSR, Ser. Khim.* **1992**, *6*, 1390–1392, Russian; *Chem. Abstr.* **1993**, *118*, 124090d.
- (56) McCrone, W. C. In *Physics and Chemistry of the Organic Solid State*; Fox, D., Labes, M. M., Weissberger, A., Eds.; Interscience: New York, 1965; Vol. 2, pp 725–767.
- (57) Sheldrick, G. M. *SHELXTL PC, Ver. 4.1 An Integrated System for Solving, Refining and Displaying Crystal Structure from Diffraction Data*; Siemens Analytical X-ray Instruments, Inc.: Madison, WI, 1990.
- (58) At room temperature, the unit cell parameters were as follows (the same crystals as for the low-temperature experiments were used): H<sub>2</sub>L, stable form (275 reflections):  $a = 10.147(3)$  Å,  $b = 7.624(3)$  Å,  $c = 12.258(4)$  Å,  $\beta = 103.92(2)^\circ$ ,  $V = 920.4(5)$  Å<sup>3</sup>,  $d = 1.336$  g cm<sup>-3</sup> (for  $Z = 2$ ). H<sub>2</sub>L, metastable form (140 reflections):  $a = 12.104(4)$  Å,  $b = 3.950(1)$  Å,  $c = 38.39(1)$  Å,  $\beta = 97.61(2)^\circ$ ,  $V = 1819.3(9)$  Å<sup>3</sup>,  $d = 1.352$  g cm<sup>-3</sup> (for  $Z = 4$ ). See Supporting Information for more details.
- (59) Grachev, E. V.; Dyadin, Yu. A.; Lipkowski, J. *J. Struct. Chem.* **1995**, *36*, 876–879.
- (60) Bondi, A. *J. Phys. Chem.* **1964**, *68*, 441–451.
- (61) Zefirov, Yu. V.; Zorkii, P. M. *Russ. Chem. Rev.* **1995**, *64*, 415–428.
- (62) Williams, D. E. *Acta Crystallogr.* **1966**, *21*, 340–349.
- (63) Templeton, D. H.; Zalkin, A. *Acta Crystallogr.* **1973**, *B29*, 1552–1553.
- (64) Jones, R. D. G. *Acta Crystallogr.* **1976**, *B32*, 1807–1811.
- (65) Etter, M. C.; Jahn, D. A.; Urbani czyk-Lipkowska, Z. *Acta Crystallogr.* **1987**, *C43*, 260–263.
- (66) Williams, D. E.; Dumke, W. L.; Rundle, R. E. *Acta Crystallogr.* **1962**, *15*, 627–635.
- (67) Engebretson, G. R.; Rundle, R. E. *J. Am. Chem. Soc.* **1964**, *86*, 574–581.
- (68) Soldatov, D. V.; Henegouwen, A. T.; Enright, G. D.; Ratcliffe, C. I.; Ripmeester, J. A. *Inorg. Chem.* **2001**, *40*, 1626–1636.
- (69) Hunter, C. A.; Sanders, J. K. M. *J. Am. Chem. Soc.* **1990**, *112*, 5525–5534.

- (70) CSD version 5.24 (November 2002).
- (71) Talberg, H. J. *Acta Chem. Scand.* **1978**, A32, 375–376.
- (72) Vishnumurthy, K.; Row, T. N. G.; Venkatesan, K. *Tetrahedron* **1999**, 55, 4095–4108.
- (73) Attar, S.; Forkey, D. M.; Olmstead, M. M.; Balch, A. L. *Chem. Commun.* **1998**, 1255–1256.
- (74) Miljkovic, A.; Mantle, P. G.; Williams, D. J.; Rassing, B. J. *Nat. Prod.* **2001**, 64, 1251–1253.
- (75) Kemula, W.; Lipkowski, J.; Sybilska, D. *Rocz. Chem.* **1974**, 48, 3–12.
- (76) Soldatov, D. V.; Grachev, E. V.; Ripmeester, J. A. *Cryst. Growth Des.* **2002**, 2, 401–408.
- (77) Abrahams, B. F.; Jackson, P. A.; Robson, R. *Angew. Chem., Int. Ed. Engl.* **1998**, 37, 2656–2659.
- (78) Li, H.; Eddaoudi, M.; O’Keeffe, M.; Yaghi, O. M. *Nature* **1999**, 402, 276–279.
- (79) Kondo, M.; Shimamura, M.; Noro, S.; Minakoshi, S.; Asami, A.; Seki, K.; Kitagawa, S. *Chem. Mater.* **2000**, 12, 1288–1299.
- (80) Fletcher, A. J.; Cussen, E. J.; Prior, T. J.; Rosseinsky, M. J.; Kepert, C. J.; Thomas, K. M. *J. Am. Chem. Soc.* **2001**, 123, 10001–10011.
- (81) Cussen, E. J.; Claridge, J. B.; Rosseinsky, M. J.; Kepert, C. J. *J. Am. Chem. Soc.* **2002**, 124, 9574–9581.
- (82) Lu, J. Y.; Babb, A. M. *Chem. Commun.* **2002**, 1340–1341.
- (83) Noro, S.; Kitaura, R.; Kondo, M.; Kitagawa, S.; Ishii, T.; Matsuzaka, H.; Yamashita, M. *J. Am. Chem. Soc.* **2002**, 124, 2568–2583.
- (84) Uemura, K.; Kitagawa, S.; Kondo, M.; Fukui, K.; Kitaura, R.; Chang, H.-C.; Mizutani, T. *Chem. Eur. J.* **2002**, 8, 3586–3600.
- (85) Seki, K. *Phys. Chem. Chem. Phys.* **2002**, 4, 1968–1971.
- (86) Atwood, J. L.; Barbour, L. J.; Jerga, A.; Schottel, B. L. *Science* **2002**, 298, 1000–1002.
- (87) Kitagawa, S.; Kondo, M. *Bull. Chem. Soc. Jpn.* **1998**, 71, 1739–1753.
- (88) Soldatov, D. V.; Ripmeester, J. A.; Shergina, S. I.; Sokolov, I. E.; Zanina, A. S.; Gromilov, S. A.; Dyadin, Yu. A. *J. Am. Chem. Soc.* **1999**, 121, 4179–4188.
- (89) Halder, G. J.; Kepert, C. J.; Moubaraki, B.; Murray, K. S.; Cashion, J. D. *Science* **2002**, 298, 1762–1765.
- (90) Kim, I.; Kwak, B.; Lah, M. S. *Inorg. Chim. Acta* **2001**, 317, 12–20.
- (91) Müller, P.; Usón, I.; Hensel, V.; Schlüter, A. D.; Sheldrick, G. M. *Helv. Chim. Acta* **2001**, 84, 778–785.
- (92) Mena-Osteritz, E.; Bäuerle, P. *Adv. Mater.* **2001**, 13, 243–246.
- (93) Su, C.-Y.; Yang, X.-P.; Kang, B.-S.; Mak, T. C. W. *Angew. Chem., Int. Ed.* **2001**, 40, 1725–1728.
- (94) Zhao, D.; Moore, J. S. *J. Org. Chem.* **2002**, 67, 3548–3554.
- (95) Campbell, K.; Kuehl, C. J.; Ferguson, M. J.; Stang, P. J.; Tykwinski, R. R. *J. Am. Chem. Soc.* **2002**, 124, 7266–7267.
- (96) Abourahma, H.; Moulton, B.; Kravtsov, V.; Zaworotko, M. J. *J. Am. Chem. Soc.* **2002**, 124, 9990–9991.

CG030016B